International Journal of Research in Advent Technology, Vol.6, No.9, September 2018
E-ISSN: 2321-9637
Available online at www.ijrat.org

Entropy Generation of Oldroyd-B Fluid through various Geometrical Structures

Debasish Dey [1], Ardhendu Sekhar Khound [2]
Assistant Professor, Department of Mathematics, Dibrugarh University, Dibrugarh-786 004, Assam.[1]
Research Scholar, Department of Mathematics, Dibrugarh University, Dibrugarh-786 004, Assam[2]
Email: debasish41092@gmail.com[1], *ardhendu.khound@gmail.com*[2]

Abstract- In this paper, the entropy generation rate in unsteady visco-elastic Oldroyd-B through various geometrical structures has been investigated. Here we study the effect of relaxation parameter, retardation parameter, thermal conductivity, magnetic parameter, gravitational parameter etc on entropy generation. We also compare the entropy generation rate of non Newtonian fluid with the Newtonian fluid. The results are discussed graphically for various flow parameters involved in the solution.

Keywords- Relaxation and retardation, Oldroyd-B fluid model, entropy generation, Shearing stress.

1. INTRODUCTION:

In today's world many researchers and scientists are attracted towards the mechanism of visco-elastic fluid flow due to their use in various industries such as polymer solution, suspension, paints, cosmetic products etc. To study the flow pattern of visco-elastic fluid flow Oldroyd [1, 2] have proposed the constitutive equation of fluid model and is named as Oldroyd fluid model. The model is given by

$$\sigma_{ij} = -p\delta_{ij} + \tau_{ij},$$

$$\left(1 + \lambda_1 \frac{d}{dt}\right)\tau_{ij} = 2\mu\left(1 + \lambda_2 \frac{d}{dt}\right)e_{ij} \qquad (1)$$

where p hydrostatic pressure, σ_{ij} stress tensor, τ_{ij} viscous-stress tensor, δ_{ij} kronecker delta, λ_1 relaxation time, λ_2 retardation time, e_{ij} is strain tensor, μ co-efficient of viscosity and $\frac{d}{dt}$ is material derivative.

Demirel and Kahraman [3] have investigated the thermodynamic analysis of convective heat transfer in an annular packed bed. Mahmud and Fraser [4] have studied the inherent irreversibility of channel and pipe flows for non-newtonian fluids. Yilbas *et al.* [5] have investigated the entropy analysis for non- newtonian fluid flow in annular pipe: constant viscosity case. Entropy generation in double diffusive in presence of soret effect has been studied by Hidouri *et al.* [6]. Magherbi *et al.* [7] have examined the influence of Dufour effect on entropy generation in double diffusive convection. The entropy generation due to non-newtonian fluid flow in annular pipe with relative rotation: constant viscosity case has been studied by Ali and Muhammet [8]. The effects of radiation heat transfer on entropy generation at thermosolutal convection in a square cavity subjected to a magnetic field have been examined by Hidouri *et al.* [9]. Makinde and Eegunjobi [10] have investigated the effects of convective heating on entropy generation rate in a channel with permeable walls. Heat and mass transfer of MHD second order slip flow has been studied by Turkyilmazoglu [11]. Das and Jana [12] examined the entropy generation due to MHD flow in a porous channel with slip at the surface. Adesanya and Falade [13] have analyzed thermodynamics analysis of hydromagnetic third grade fluid flow through a channel filled with porous medium. Chen *et al.* [14] studied the entropy generation in mixed convection mag-netohydrodynamic nanofluid flow in vertical channel. Entropy generation analysis for a reactive couple stress fluid flow through a channel saturated with porous material has been examined by Adesanya *et al.* [15]. Also second law analysis of buoyancy driven unsteady channel flow of nano-fluids with convective cooling has been investigated by Mkwizu *et al.* [16]. Dey and Khound [17, 18, 20] have analyzed the relaxation and retardation effects on free convective visco-elastic fluid flow governed by of Oldroyd-B model. Kareem *et al.* [19] have studied the entropy generation rate in unsteady buoyancy-driven hydromagnetic couple stress fluid flow through a porous channel.

The objective of the work is to investigate the entropy generation guided by Oldroyd fluid flow in three cases: (i) Flow through an oscillating surface (Dey and Khound [17]) (ii) Flow though a porous channel (Dey and Khound [18]) (iii) Flow though an oscillating porous belt (Dey and Khound [20]). Also, the work will guide to find out the factors responsible for enhancing entropy generation.

2. MATHEMATICAL FORUMULATIONS:

Time dependent fluid flow directed by Oldroyd-B fluid model has been considered with

free convection and transverse magnetic field. Along with pressure gradient, other forces govern the fluid motion are (i) viscous force (ii) Buoyancy force (iii) Lorentz force etc. Buoyancy force leads to free convection and applying Boussinesq approximation (variation of density in inertia term), equation of state and free stream conditions, pressure gradient term is replaced by free convection terms. Application of transverse magnetic field, generates Lorentz force and the force per unit volume is given by $\vec{j} \times \vec{B}$ ($\vec{j} = \sigma(\vec{v} \times \vec{B})$, σ electrical conductivity, $\vec{v}$ fluid velocity, $\vec{B}$ magnetic field). Gauss's law magnetism states that $\vec{B} = (0, \boldsymbol{B_0}, 0)$. The magnetic Reynolds number is taken to be small and hence induced magnetic is neglected. In the mixture, one of the components is assumed to be rarer lighter, let C_1 and C_2 be the concentrations of lighter and heavier components respectively and C_2 (C')= 1- C_1. The motion of binary mixture is similar to normal fluid flow with velocity $u' = \frac{u_1\rho_1 + u_2\rho_2}{\rho_1 + \rho_2}$ and density $\rho = \rho_1 + \rho_2$, where ρ_1, ρ_2, u_1 & u_2 are densities and velocities of rarer and heavier components respectively.

2.1 Flow through an Oscillating Surface:

In this case, we have extended the work [17] by analyzing entropy generation. Geometry of the problem is given by figure 2.1. Geometry reveals that the x' axis coincides with the length of the surface and y' axis is along the transverse direction.

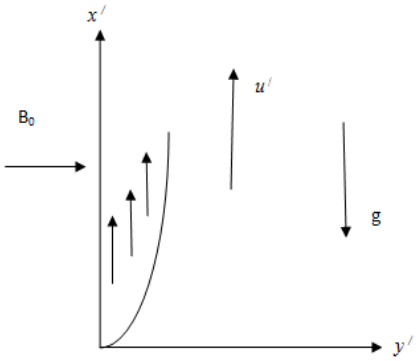

Figure 2.1: Geometry of the Problem

In this problem we used the following non-dimensional quantities.

$$y = \frac{U_0 y'}{\nu}, u = \frac{u'}{U_0}, t = \frac{t' U_0^2}{\nu}, \theta = \frac{T' - T_\infty}{T_w - T_\infty},$$
$$\phi = \frac{C' - C_\infty}{C_w - C_\infty}, a = \lambda_1 \frac{U_0^2}{\nu}, b = \lambda_2 \frac{U_0^2}{\nu}, M = \frac{\sigma B_0^2 \nu}{\rho U_0^2}$$
$$G_r = \frac{g\beta(T_w - T_\infty)}{\rho U_0^3}, G_m = \frac{g\beta^*(C_w - C_\infty)}{\rho U_0^3},$$
$$Sc = \frac{\nu}{D}, Pr = \frac{\mu c_p}{K}, E_T = \frac{kU_0^2(T_w - T_\infty)^2}{{T_\infty}^2 \nu^2},$$
$$E_{SH} = \frac{\mu U_0^4 \rho}{T_\infty \nu}, E_C = \frac{DU_0^2(C_w - C_\infty)^2}{{C_\infty}^2 \nu^2},$$
$$, E_{TC} = \frac{DU_0^2(T_w - T_\infty)^2(C_w - C_\infty)^2}{T_\infty \nu},$$
$$E_M = \frac{\sigma B_0^2 U_0^2}{T_\infty} \quad (2)$$

into the Momentum equation, Energy equation and Energy equation for species concentration of Dey and Khound [17] and we get following set of dimensionless equations,

$$\frac{\partial u}{\partial t} + a\frac{\partial^2 u}{\partial t^2} = \left[1 + a\frac{\partial}{\partial t}\right][G_r\theta + G_m\phi] + \frac{\partial^2 u}{\partial y^2} + b\frac{\partial^3 u}{\partial y^2 \partial t} - \left[1 + a\frac{\partial}{\partial t}\right]Mu \quad (3)$$

$$Pr\frac{\partial \theta}{\partial t} = \frac{\partial^2 \theta}{\partial y^2} \quad (4)$$

$$Sc\frac{\partial \phi}{\partial t} = \frac{\partial^2 \phi}{\partial y^2} \quad (5)$$

The relevant boundary conditions for solving the equations (3) to (5) are as follows:

$$y = 0, u = 1 + \epsilon e^{i\omega t}, \theta = \epsilon e^{i\omega t}, \phi = \epsilon e^{i\omega t} \;\&\; y \to \infty, u \to 0, \theta \to 0, \phi \to 0 \quad (6)$$

The boundary condition reveals that the surface is characterized by an oscillation with mean velocity U_0

2.2 Flows through a porous channel:

Here we consider unsteady binary mixture free convective visco-elastic fluid flow through a porous channel with Hall current effects. Geometry of the figure is given by figure 2.2

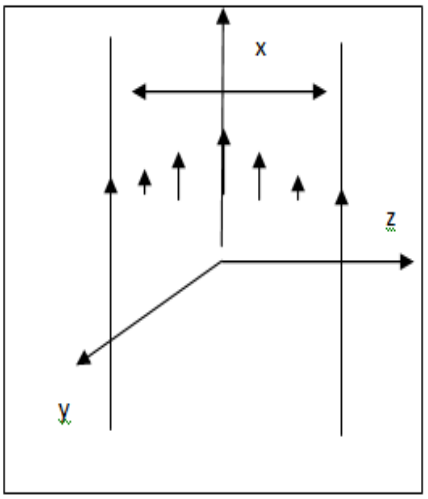

Figure 2.2: Geometry of the Problem

Here we use the following non-dimensional quantities into the momentum equation, energy equation and concentration equation of Dey and Khound [18] to make them dimensionless.

$$x=\frac{x'}{d};y=\frac{y'}{d};z=\frac{z'}{d};\ u=\frac{u'}{U};v=\frac{v'}{U};$$
$$t=\frac{t'U}{d};p=\frac{p*}{\rho U^2};\omega=\frac{\omega' d}{U};T=\frac{T'-T_0}{T_w-T_0};$$
$$C=\frac{C'-C_0}{C_w-C_0};a=\frac{\lambda_1 U}{d};b=\frac{\lambda_2 U}{d};$$
$$M=\frac{\sigma B_0^2 d^2}{\upsilon};\ G_r=\frac{g\beta d^2(T_w-T_0)}{\nu U};$$
$$G_m=\frac{g\beta^* d^2(C_w-C_0)}{\nu U};\ Re=\frac{Ud}{\nu};$$
$$Pe=\frac{\rho C_p U d}{k};\ N=\frac{2\alpha d}{\sqrt{k}};h=\frac{d^2 k_1}{D};$$
$$k_p=\frac{k'_p}{d};m=\omega_e\tau_e;E_T=\frac{k(T_w-T_0)^2}{{T_w}^2 d^2},$$
$$E_{SH}=\frac{\mu^2 U^2\rho}{T_w d^2},E_C=\frac{D(C_w-C_0)^2}{{C_w}^2 d^2},$$
$$E_{TC}=\frac{D(T_w-T_0)(C_w-C_0)}{T_w d^2},$$
$$E_M=\frac{\sigma B_0^2 U^2}{T_w} \qquad (7)$$

The dimensionless equations are as follows:

$$Re\left(\frac{\partial u}{\partial t}+a\frac{\partial^2 u}{\partial t^2}\right)=-Re\left(1+a\frac{\partial}{\partial t}\right)\frac{\partial p}{\partial x}+\frac{\partial^2 u}{\partial z^2}$$
$$+b\frac{\partial^3 u}{\partial z^2\partial t}+\left(1+a\frac{\partial}{\partial t}\right)\left[M\left(\frac{mv-u}{1+m^2}\right)-\frac{u}{k_p}+G_r T+G_m C\right] \qquad (8)$$

$$Re\left(\frac{\partial v}{\partial t}+a\frac{\partial^2 v}{\partial t^2}\right)=-Re\left(1+a\frac{\partial}{\partial t}\right)\frac{\partial p}{\partial y}+\frac{\partial^2 v}{\partial z^2}$$
$$+b\frac{\partial^3 v}{\partial z^2\partial t}+\left(1+a\frac{\partial}{\partial t}\right)\left[-M\left(\frac{mu+v}{1+m^2}\right)-\frac{v}{k_p}\right] \qquad (9)$$

$$Pe\frac{\partial T}{\partial t}=\frac{\partial^2 T}{\partial z^2}-N^2 T \qquad (10)$$

$$Sc\frac{\partial C}{\partial t}=\frac{\partial^2 C}{\partial z^2}-hC \qquad (11)$$

Equations (8) and (9) can be combined into a single differential equation by assuming $F=u+iv$ and we get,

$$Re\left(1+a\frac{\partial}{\partial t}\right)\left(\frac{\partial F}{\partial t}+\frac{\partial p}{\partial x}+i\frac{\partial p}{\partial y}\right)$$
$$=\frac{\partial^2 F}{\partial z^2}+b\frac{\partial^3 F}{\partial z^2\partial t}$$
$$+\left(1+a\frac{\partial}{\partial t}\right)\left[\frac{-MF(1+im)}{1+m^2}-\frac{F}{k_p}+G_r T+G_m C\right] \qquad (12)$$

Following ([21 & 22]), the pressure gradient of the oscillatory flow is taken as $\frac{\partial p}{\partial x}=-Ae^{i\omega t},\frac{\partial p}{\partial y}=0$

To solve the above equations from (10) to (12) the following boundary conditions are used

$$T=C=F=0;z=-\frac{1}{2}\ \&$$
$$T=C=e^{i\omega t};F=0;\ z=\frac{1}{2} \qquad (13)$$

2.3 Flows through an Oscillating Inclined Belt

In this case an unsteady thin film flow of visco-elastic fluid characterized by Oldroyd-B fluid model consisting of nano-sized particles through an inclined belt has been examined. The lower surface of the belt is oscillating about a non-zero constant mean velocity U. Outer surface is characterized by convection-conduction and convection-diffusion boundary conditions. The motion of the fluid layer is in downward direction due to the influence of gravitational force g. Let x' axis be taken along the length of belt (infinite in length) and y' axis be taken perpendicular to it. Governing equations of motion are solved analytically by using perturbation scheme. Geometry of the case is given by figure 2.3

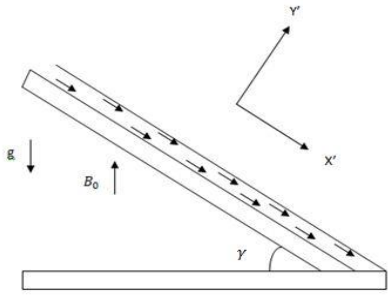

Figure 2.3: Geometry of the case

We introduce the following non-dimensional quantities to make the equations momentum equation, temperature equation and concentration equation in Dey and Khound [20] dimensionless:

$$y=\frac{y'}{\delta};\ u=\frac{u'}{U};\ t=\frac{\mu t'}{\rho\delta};\ \theta=\frac{T'-T_S}{T_0-T_S};$$
$$\phi=\frac{C'-C_S}{C_0-C_S};\ a=\frac{\lambda_1\mu}{\rho\delta^2};\ b=\frac{\lambda_2\mu}{\rho\delta^2};$$
$$M=\frac{\sigma {B_0}^2\delta^2}{\mu};\ \omega=\frac{\omega'\rho\delta^2}{\mu};m=\frac{\rho\delta^2 g\sin\gamma}{\mu U};$$
$$Sc=\frac{\mu}{\rho D_b};Pr=\frac{\mu}{\rho\alpha};N_b=\frac{\rho^2 D_b(C_0-C_S)}{\mu(T_0-T_S)};$$
$$E_T=\frac{k(T_0-T_s)^2}{{T_s}^2\delta};\ E_{SH}=\frac{\mu f_0^2\rho}{T_s\delta},$$

$$E_C = \frac{D(C_0 - C_s)^2}{{C_s}^2 \delta}, E_{TC} = \frac{D(T_0 - T_s)(C_0 - C_s)}{T_s \delta^2}$$

$$E_M = \frac{\sigma B_0^2 U^2}{T_s} \quad (14)$$

The dimensionless equations are as follows:

$$\frac{\partial u}{\partial t} + a\frac{\partial^2 u}{\partial t^2} = \frac{\partial^2 u}{\partial y^2} + b\frac{\partial^3 u}{\partial y^2 \partial t} - \left[1 + a\frac{\partial}{\partial t}\right] Mu + m \quad (15)$$

$$\frac{\partial \theta}{\partial t} = \frac{1}{Pr}\frac{\partial^2 \theta}{\partial y^2} + N_b \frac{\partial \theta}{\partial y}\frac{\partial \phi}{\partial y} \quad (16)$$

$$Sc\frac{\partial \phi}{\partial t} = \frac{\partial^2 \phi}{\partial y^2} \quad (17)$$

We use the following boundary conditions for solving the equations (15) to (17):

$$y = 0, u = 1 + \epsilon e^{i\omega t}, \theta = \epsilon e^{i\omega t}, \phi = \epsilon e^{i\omega t} \;\&\; y = 1, \frac{\partial u}{\partial y} = 0, \theta = \frac{\delta h_f}{k} = Nc, \phi = \frac{\delta h_m}{D_b} = Nd \quad (18)$$

3. RESULTS AND DISCUSSIONS:

3.1 CASE I:

The rate of entropy generation is given by:

$$S'_{gen} = \frac{K}{{T_\infty}^2}\left(\frac{\partial T'}{\partial y'}\right)^2 + \frac{\mu}{T_\infty}\left(\tau\frac{\partial u'}{\partial y'}\right)^2 + \frac{D}{{C_\infty}^2}\left(\frac{\partial C'}{\partial y'}\right)^2 + \frac{D}{T_\infty}\left(\frac{\partial T'}{\partial y'}\right)\left(\frac{\partial C'}{\partial y'}\right) + \frac{\sigma B_0^2}{T_\infty}u'^2 \quad (19)$$

Using the non-dimensional parameters in (2) we get the dimensionless rate of entropy generation is

$$S_{gen} = E_T\left(\frac{\partial \theta}{\partial y}\right)^2 + E_{SH}\left(\tau\frac{\partial u}{\partial y}\right)^2 + E_C\left(\frac{\partial \phi}{\partial y}\right)^2 + E_{TC}\left(\frac{\partial \theta}{\partial y}\right)\left(\frac{\partial \phi}{\partial y}\right) + E_M u^2 \quad (20)$$

In the figure (3.1.1) we see that during the growth of the relaxation parameter 133% (approximate) (from a=1.5 to a=3.5), there is an increment in entropy generation by 20% (approximate). Also it is noticed from figure (3.1.2) that the entropy generation rate is increased by 40% (approximate) during the increment in retardation by 27% which is noticed in figure (3.1.2). Figure 3.1.3 notifies that the wastage or entropy is seen more in non-Newtonian fluid flow than Newtonian fluid flow.

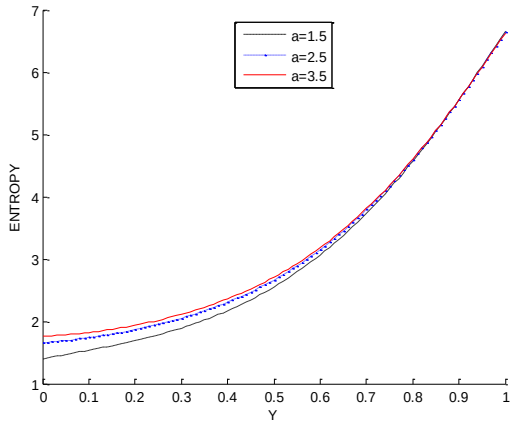

Figure 3.1.1: Entropy against y for b=1.5, E_T=4, E_{SH}=0.5, E_C=3, E_{TC}=2, E_M=2.5, M=0.1, Pr=0.5, Sc=1, ω=5, t=0.1, G_r=7, G_m=3, ϵ=0.1

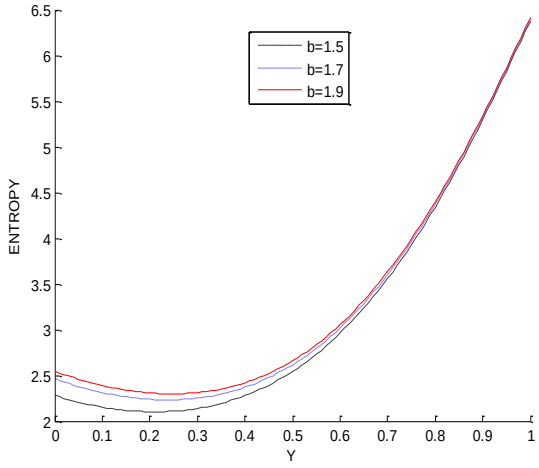

Figure 3.1.2: Entropy against y for a=0.5, E_T=4, E_{SH}=0.5, E_C=3, E_{TC}=2, E_M=2.5, M=0.1, Pr=0.5, Sc=1, ω=5, t=0.1, G_r=7, G_m=3, ϵ=0.1

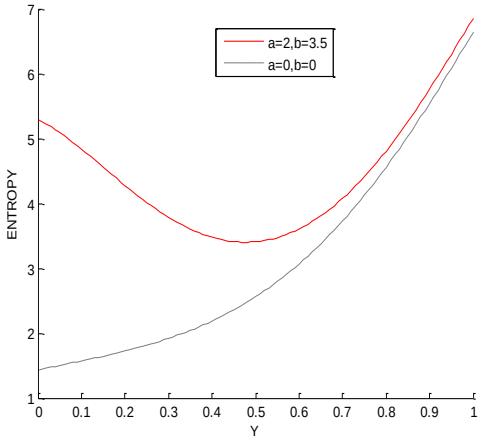

Figure 3.1.3: Entropy against y for E_T=4, E_{SH}=0.5, E_C=3, E_{TC}=2, E_M=2.5, M=0.1, Pr=0.5, Sc=1, ω=5, t=0.1, G_r=7, G_m=3, ϵ=0.1

3.2. CASE II

The rate of entropy generation is given by:

$$S'_{gen} = \frac{K}{{T_w}^2}\left(\frac{\partial T'}{\partial z'}\right)^2 + \frac{\mu}{T_w}\left(\tau_{xz}'\frac{\partial u'}{\partial z'} + \tau_{yz}'\frac{\partial v'}{\partial z'}\right)^2 + \frac{D}{{C_w}^2}\left(\frac{\partial C'}{\partial z'}\right)^2 + \frac{D}{T_w}\left(\frac{\partial T'}{\partial z'}\right)\left(\frac{\partial C'}{\partial z'}\right) + \frac{\sigma B_0^2(u'^2+v'^2)}{T_w} \quad (21)$$

Using the above mentioned non-dimensional parameters in (7) we get the dimensionless rate of change

$$S_{gen} = E_T\left(\frac{\partial T}{\partial z}\right)^2 + E_{SH}\left(\tau_{xz}\frac{\partial u}{\partial z} + \tau_{yz}\frac{\partial v}{\partial z}\right)^2 + E_C\left(\frac{\partial C}{\partial z}\right)^2 + E_{TC}\left(\frac{\partial T}{\partial z}\right)\left(\frac{\partial C}{\partial z}\right) + E_M(u^2+v^2) \quad (22)$$

In the figure (3.2.1) and (3.2.2) we noticed that the relaxation and retardation parameters have positive impact on entropy generation. Thus it may be concluded that to reduce the entropy, relaxation and retardation parameters should be controlled. The entropy generation rate is 15.43% (approximate) more in non-Newtonian fluid as compared to that of Newtonian fluid as we see in figure (3.2.3).

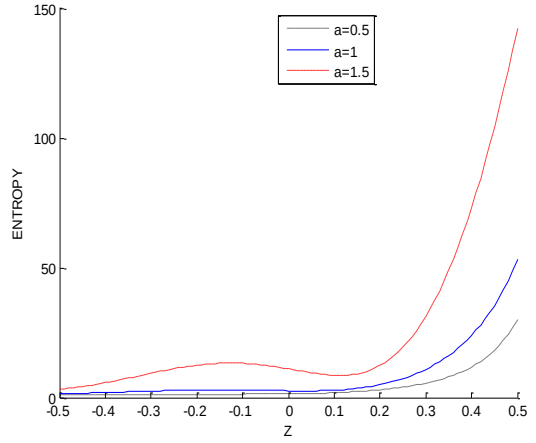

Figure 3.2.1: Entropy against y for b=1.2, ω=0.01, A=-0.5, M=2, Re=0.3, Pe=8, N=8, Gm=4, Gr=7, h=0.5, Sc=2, kp=0.2, m=1, t=2, E_T=0.2, E_{SH}=0.5, E_C=0.7, E_{TC}=0.8, E_{UV}=0.3

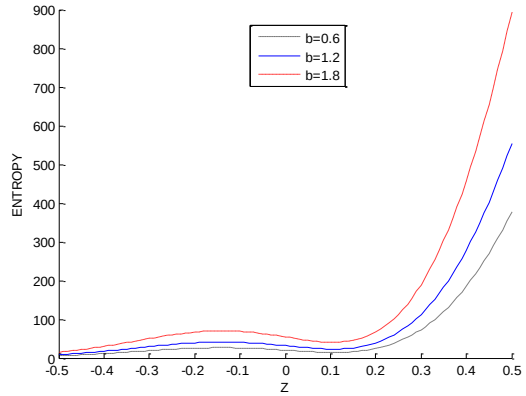

Figure 3.2.2: Entropy against y for a=1.5, ω=0.01, A=-0.5, M=2, Re=0.3, Pe=8, N=8, Gm=4, Gr=7, h=0.5, Sc=2, kp=0.2, m=1, t=2, E_T=0.2, E_{SH}=0.5, E_C=0.7, E_{TC}=0.8, E_{UV}=0.3

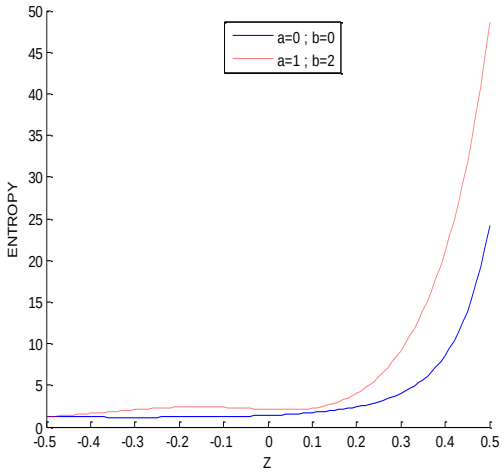

Figure 3.2.3: Entropy against y for ω=0.01, A=-0.5, M=2, Re=0.3, Pe=8, N=8, Gm=4, Gr=7, h=0.5, Sc=2, kp=0.2, m=1, t=2, E_T=0.2, E_{SH}=0.5, E_C=0.7, E_{TC}=0.8, E_{UV}=0.3

3.3. CASE III

The rate of entropy generation is given by:

$$S'_{gen} = \frac{K}{{T_s}^2}\left(\frac{\partial T'}{\partial y'}\right)^2 + \frac{\mu}{T_s}\left(\tau'\frac{\partial u'}{\partial y'}\right)^2 + \frac{D}{{C_s}^2}\left(\frac{\partial C'}{\partial y'}\right)^2 + \frac{D}{T_s}\left(\frac{\partial T'}{\partial y'}\right)\left(\frac{\partial C'}{\partial y'}\right) + \frac{\sigma B_0^2}{T_s}u'^2 \quad (23)$$

Using the above mentioned non-dimensional parameters in (14) we get the dimensionless rate of change

$$S_{gen} = E_T\left(\frac{\partial \theta}{\partial y}\right)^2 + E_{SH}\left(\tau\frac{\partial u}{\partial y}\right)^2 + E_C\left(\frac{\partial \phi}{\partial y}\right)^2 + E_{TC}\left(\frac{\partial \theta}{\partial y}\right)\left(\frac{\partial \phi}{\partial y}\right) + E_M u^2 \quad (24)$$

When thermal conductivity increase by 800% (from k=0.5 to k=4.5) the entropy generation rate is decreased by 10% (approximate) as we notice in the figure (3.3.1). It is due to the fact that the growth in thermal conductivity results in the increase in heat transfer and as a consequence entropy generation rate enhances. When magnetic parameter increases by 200% the entropy generation rate is decreased by 7% (approximate) (figure 3.3.2). The entropy generation rate is increased by 0.5% (approximate) when the gravitational parameter increases by 40% (figure 3.3.3). Table 3.1 and 3.2 reflect the effects of relaxation and retardation parameters on entropy generation across the flow. It may be concluded that entropy generation experiences upward trend with

the rise of relaxation and retardation time parameters.

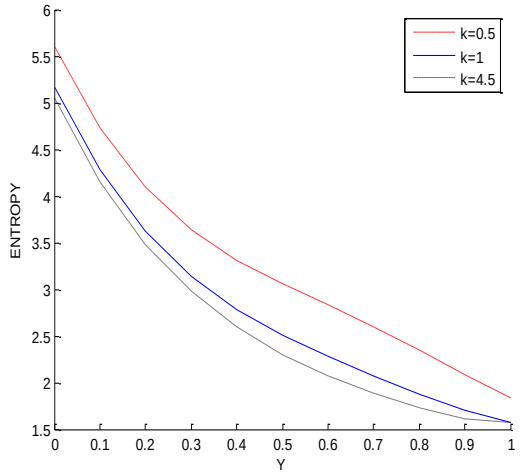

Figure 3.3.1: Entropy against y for a=0.2, b=0.3, M=2, Pr=5, h_f=.4, N_b=0.05, h_m=3, m=4, D_b=2, d=1, Sc=0.3, ω=2, ϵ=0.001, t=1, E_T=0.2, E_C=0.3, E_{SH}=2, E_{TC}=0.3, E_U=0.5

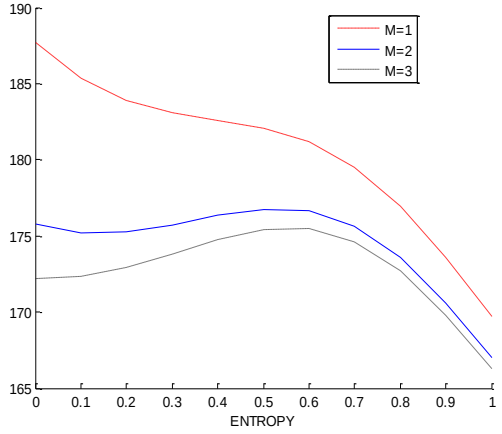

Figure 3.3.2: Entropy against y for a=0.2, b=0.3, Pr=5, k=0.03, m=4, h_f=0.4, N_b=0.05, h_m=3, D_b=2, d=1, Sc=0.3, ω=2, ϵ=0.001, t=1, E_T=0.2, E_C=0.3, E_{SH}=2, E_{TC}=0.3, E_U=0.5

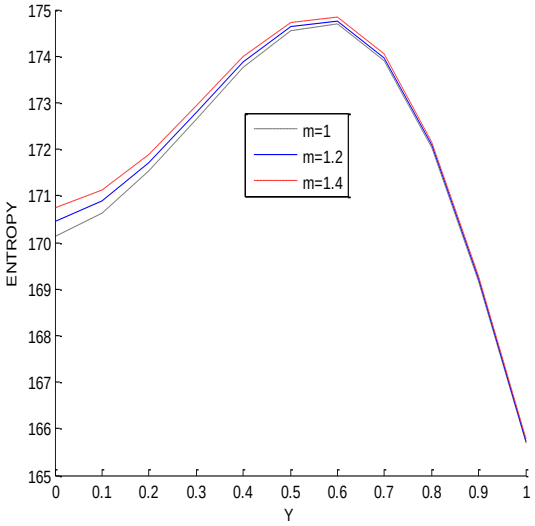

Figure 3.3.3: Entropy against y for a=0.2, b=0.3, M=2, Pr=5, k=0.03, h_f=0.4, N_b=0.05, h_m=3, D_b=2, d=1, Sc=0.3, ω=2, ϵ=0.001, t=1, E_T=0.2, E_C=0.3, E_{SH}=2, E_{TC}=0.3, E_U=0.5

y	a=0.6, b=0.3	a=0.8, b=0.3	a=1, b=0.3
0.0	172.2318	172.2332	172.2355
0.2	172.9259	172.9263	172.9271
0.4	174.7649	174.7651	174.7653
0.6	175.4910	175.4911	175.4911
0.8	172.7273	172.7275	172.7275
1	166.3001	166.3002	166.3003

Table 3.1: Entropy for M=2, Pr=5, h_f=.4, N_b=0.05, h_m=3, k=0.03, m=4, D_b=2, d=1, Sc=0.3, ω=2, ϵ=0.001, t=1, E_T=0.2, E_C=0.3, E_{SH}=2, E_{TC}=0.3, E_U=0.5.

y	a=0.6, b=0.9	a=0.6, b=1.1	a=0.6, b=1.3
0.0	172.2359	172.2361	172.2362
0.2	172.9273	172.9274	172.9274

0.4	174.7651	174.7652	174.7652
0.6	175.4907	175.4907	175.4907
0.8	172.7269	172.7269	172.7269
1	166.2997	166.2997	166.2997

Table 3.2: Entropy for M=2, Pr=5, h_f=.4, N_b=0.05, h_m=3, k=0.03, m=4, D_b=2, d=1, Sc=0.3, ω=2, ϵ=0.001, t=1, E_T=0.2, E_C=0.3, E_{SH}=2, E_{TC}=0.3, E_U=0.5.

REFERENCES

[1] J. G. Oldroyd. "On the Formulation of Rheological Equations of State". Proceedings of the Royal Society of London. Series A, Mathematical and Physical Sciences, 200 (1063): 523–541, 1950.

[2] J. G. Oldroyd. "Non-Newtonian effects in steady motion of some idealized elastic-viscous liquids". Proc. Roy. Soc. Lond., A245: 278-297, 1958.

[3] Y. Demirel and R. Kahraman. "Thermodynamic analysis of convective heat transfer in an annular packed bed". International Journal of Heat and Fluid Flow, 21: 442-448, 2000.

[4] S. Mahmud and R.A. Fraser. "Inherent irreversibility of channel and pipe flows for non-Newtonian fluids" Int. Comm. Heat Mass Transfer, 29: 577-587, 2002.

[5] B. S. Yilbas, M. Y¨ur¨usoy and M Pakdemirli. "Entropy analysis for non- Newtonian fluid flow in annular pipe: Constant viscosity case". Entropy, 304-315, 2004.

[6] N. Hidouri, M. Magherbi, H. Abbassi and A. Ben Brahim. "Entropy generation in double diffusive in presence of Soret effect". Prog. Comput. Fluid Dyn, 5: 237–246, 2007.

[7] M. Magherbi, N. Hidouri, H. Abbassi and A. Ben Brahim. "Influence of Dufour effect on entropy generation in double diffusive convection". Int. J. Exergy, 4: 227–252, 2007.

[8] K. Ali and Y. Muhammet. "Entropy Generation Due To Non-Newtonian Fluid Flow In Annular Pipe With Relative Rotation: Constant Viscosity Case". Journal Of Theoretical And Applied Mechanics, 46(1): 69-83, 2008.

[9] N. Hidouri, M. Bouabid, M. Magherbi and A. B. Brahim. "Effects of Radiation Heat Transfer on Entropy Generation at Thermosolutal Convection in a Square Cavity Subjected to a Magnetic Field". Entropy, 13: 1992-2012, 2011, doi:10.3390/e13121992.

[10] O. D. Makinde and A. S. Eegunjobi. "Effects of convective heating on entropy generation rate in a channel with permeable Walls". Entropy, 15: 220-233, 2013.

[11] M. Turkyilmazoglu. "Heat and mass transfer of MHD second order slip flow". Computers & Fluids, 71: 426–434, 2013.

[12] S. Das and R. N. Jana. "Entopy generation due to MHD flow in a porous channel with navier slip". Ain Shams Eng. J, 5: 575–584, 2014.

[13] S. O. Adesanya and J. A. Falade. "Thermodynamics analysis of hydromagnetic third grade fluid flow through a channel filled with porous medium". Alexandria Engineering Journal, 54(3): 615–622, 2015.

[14] C. K. Chen, B. S. Chen and C. C. Liu. "Entropy generation in mixed convection mag-netohydrodynamic nanofluid flow in vertical channel". International Journal of Heat and Mass Transfer, 91: 1026 – 1033, 2015.

[15] S. O. Adesanya, S. O. Kareem, J. A. Falade and S. A. Arekete. "Entropy generation analysis for a reactive couple stress fluid flow through a channel saturated with porous material". Energy, 93(1): 1239–1245, 2015.

[16] M. H. Mkwizu, O. D. Makinde and Y. Nkansah-Gyekye. "Second law analysis of buoyancy driven unsteady channel flow of nanofluids with convective cooling". Applied and Computational Mathematics, 4(3): 100–115, 2015.

[17] D. Dey and A. S. Khound. "Relaxation and retardation effects on free convective visco-elastic fluid flow past an oscillating plate". International Journal of Computer Applications, 144(9): 34-40, 2016, doi: 10.5120/ijca2016910434.

[18] D. Dey and A. S. Khound. "Hall current effects on binary mixture flow of Oldroyd-B fluid through a porous channel". International Journal Of Heat And Technology, 34(4): 687-693, 2016, doi: 10.18280/ijht.340419.

[19] S. O. Kareem, S. O. Adesanya, J. A. Falade and U. E. Vincent. "Entropy generation rate in unsteady buoyancy-driven hydromagnetic couple stress fluid flow through a porous channel". International Journal Of Pure And Applied Mathematics, 115(2): 311-326, 2017.

[20] D. Dey and A. S. Khound. "Analysis of thin-film flow of Oldroyd-B nano-fluid in an oscillating inclined belt with convective boundary conditions". International Journal of Mathematical Archive, 9(7): 142-150, 2018.

[21] K. D. Singh and R. Pathak. "Effects of slip conditions and Hall current on an oscillatory convective flow in a rotating vertical porous

channel with thermal radiation". International Journal of Applied Mathematics and Mechanics, 9: 60-77, 2013.

[22] K. D. Singh, B. P. Garg and A. K. Bansal. "Hall current effect on visco-elastic MHD oscillatory convective flow through a porous medium in a vertical channel with heat radiation". Proc Indian Natn Sci Acad, 80(2): 333-343, 2014.